

Asymmetry of the critical current and peak effect in superconducting multilayers

This article has been downloaded from IOPscience. Please scroll down to see the full text article.

2010 Supercond. Sci. Technol. 23 065019

(<http://iopscience.iop.org/0953-2048/23/6/065019>)

View [the table of contents for this issue](#), or go to the [journal homepage](#) for more

Download details:

IP Address: 195.50.1.122

The article was downloaded on 12/05/2010 at 13:05

Please note that [terms and conditions apply](#).

Библиотека БГУИР

Asymmetry of the critical current and peak effect in superconducting multilayers

S Yu Gavrillkin¹, O M Ivanenko¹, A N Lykov¹, K V Mitsen¹,
A Yu Tsvetkov¹, C Attanasio², C Cirillo² and S L Prischepa³

¹ P N Lebedev Physical Institute, Leninsky prospekt 53, 119991 Moscow, Russia

² CNR-SPIN-Salerno and Dipartimento di Fisica 'E R Caianiello', Università degli Studi di Salerno, Fisciano (Sa) I-84084, Italy

³ Belarus State University of Informatics and Radioelectronics, P Brovka Street 6, Minsk 220013, Belarus

Received 13 January 2010, in final form 18 March 2010

Published 12 May 2010

Online at stacks.iop.org/SUST/23/065019

Abstract

The critical current I_c in Nb/NbO and Nb/Pd multilayers with different periods has been investigated in parallel magnetic fields H . The $I_c(H)$ curves were measured for two opposite directions of the bias current I_{bias} (always oriented perpendicularly to the magnetic field) which causes the motion of the vortices towards the free surface of the sample and the substrate, respectively. For both directions of the current the so-called peak effect has been observed in the $I_c(H)$ dependencies but with a large difference in the absolute values of I_c for the positive and negative directions of I_{bias} . The position of the peak in the $I_c(H)$ dependencies does not depend on the direction of I_{bias} and it is shifted towards higher H values when the period of the multilayered structures is increased. These experimental results can be explained by considering the superposition of the applied magnetic field and the field induced by the transport current along the layers which, if the superconducting properties in different Nb layers are non-homogeneous, causes an asymmetric redistribution of the current. The effect is more pronounced when only one superconducting layer has different properties.

1. Introduction

One of the main sources of interest in superconducting artificial hybrids is the possibility of achieving high critical currents [1]. In these structures the influence of the non-superconducting layers is very strong because the spatial modulation of the superconducting order parameter in the direction orthogonal to the planes in both superconductor–insulator (S/I) and superconductor–normal metal (S/N) multilayers gives rise to a potential barrier for the free motion of the vortices. An interesting effect in the vortex properties of superconducting multilayers is the presence of peaks in the dependence of the critical current versus the parallel magnetic field, $I_c(H)$, as first observed by Raffy *et al* on Pb/PbBi proximity coupled multilayers [2]. Later the so-called peak effect was detected in other S/N and S/I systems [3–10].

The interpretation of the peak effect is based on matching considerations, and different models, which reveal the complicated nature of this phenomenon, have been proposed. One is based on the existence of commensurability between the period of the multilayer and the vortex lattice [11–15]. In this

case the matching field H_m (i.e. the field at which a maximum occurs in the $I_c(H)$ dependence) is expressed as [11]

$$\mu_0 H_m = \sqrt{3} \Phi_0 / 2\Lambda^2, \quad (1)$$

where Φ_0 is the flux quantum and Λ is the period of the layering. However, in some systems the values obtained experimentally for H_m do not follow the expression (1) (see, e.g. [8]). Another model considers the rearrangement of the parallel vortex system during which an increasing number of vortex chains is formed [5, 6, 16]. In this case the matching field is expressed as [5]

$$\mu_0 H_m = \sqrt{3} \Phi_0 N^2 / 2\gamma D^2, \quad (2)$$

where γ is the Ginzburg–Landau anisotropic mass ratio, D is the total sample thickness and $N = 2, 3, 4, \dots$ is related to the number of vortex chains. In this model surface effects are of great importance for the vortex rearrangement. In fact, if the surface roughness is very high the effectiveness of the Bean–Livingston surface barrier [17] is suppressed and the vortex rearrangement cannot be observed [9]. The change of the

vortex topology in an anisotropic superconductor, from rigid bars to perpendicular pancakes connected by parallel strips, can also explain the appearance of the peak effect [4]. Finally, it was shown that even vortex kinks which match with the layered structure could be a reason for the observed increase of I_c [8].

In all the above mentioned papers, the $I_c(H)$ dependence showing the peak effect has been detected and explained for only one direction of the bias current. Kadin *et al* some years ago analyzed an interesting effect in S/I multilayers [18]. They observed a marked asymmetry of the peak effect for critical currents of opposite polarities. This asymmetry reversed with the polarity of the magnetic field, which was applied in a direction parallel to the layers. However, to our knowledge, since this work nobody has experimentally studied in detail the influence of the direction of the bias current on the peak effect in superconducting multilayers. Recently, this asymmetric effect in the $I_c(H)$ dependence has been considered theoretically [19]. The approach developed was based on the numerical solution of the Ginzburg–Landau equations for multilayers by considering different superconducting properties in each layer. Such inhomogeneities cause a redistribution of the current, which results in different $I_c(H)$ dependencies in each layer. The superposition of the solutions in each layer describes both the peak effect and the asymmetry of the $I_c(H)$ curves for the opposite directions of the bias current.

In this work we have performed a systematic study of the $I_c(H)$ dependence on the direction of the applied bias current in Nb-based multilayers: Josephson coupled Nb/NbO (S/I) and proximity coupled Nb/Pd (S/N) hybrids. In these systems a change of the thickness of the non-superconducting layers results in a change of the coupling strength. Nb/Pd multilayers have a relatively high interface transparency [20, 21], which provides a strong proximity coupling. Also, palladium is a metal with a large spin susceptibility so the Pd layers in Nb/Pd systems (like insulating NbO in Nb/NbO) act as effective vortex pinning centers. The anisotropy γ in both systems is high, i.e. larger than four [8, 22] and therefore, in both systems a strong modulation of the superconducting order parameter is present. The distinctive feature of our work is the study of the vortex motion in two directions: towards the substrate and towards the free surface of the sample. This experimental situation is realized by changing the polarity of the transport current, which was always applied parallel to the sample surface and perpendicularly to the applied magnetic field.

The paper is organized as follows. In section 2 the sample preparation, characterization, and the details of the experiment are described. Section 3 is dedicated to the results obtained on Nb/NbO and Nb/Pd samples. In section 4 the model and the results of numerical calculations are described.

2. Experimental details

Nb/Pd multilayers were deposited on Si(100) substrates using a dual-source magnetically enhanced dc triode sputtering system with a movable substrate holder, which provides the possibility

of depositing several samples in a single deposition run, as described earlier [20]. The Si substrate was allowed to pass alternately over the Pd and Nb guns. Samples with different Nb and Pd thickness can be obtained by changing the time during which the substrate is exposed to the sputtered materials. The base pressure in the deposition chamber was in the 10^{-7} Torr range, with approximately 10^{-3} Torr of 99.999 purity Ar as the sputtering gas. All the samples are made of 10 bilayers and start with a Pd layer. The top Nb layer was additionally capped by a Pd layer to prevent Nb oxidation and avoid the occurrence of surface superconductivity. Samples with Nb thickness $d_{\text{Nb}} = 20$ nm and Pd thickness in the range $d_{\text{Pd}} = 1.7$ –20 nm have been studied. The interface roughness of these samples, as determined by x-ray reflectivity spectra, does not exceed a value of 1.2 nm, which, however, should be considered as an upper value [20]. In fact, measurements performed on a similar multilayer having $d_{\text{Nb}} = 19$ nm and $d_{\text{Pd}} = 2.0$ nm gave an interfacial roughness smaller than 1.0 nm [8], which shows the very good quality of the layering even in the sample with the smallest Pd thickness. Also, these values of the roughness are of the same order of magnitude as those obtained in the high-quality Nb/Pd bilayers used in a detailed investigation of the proximity effect in this system [23]. All the samples were patterned by a standard photolithographic lift-off technique. The stripes were 100 μm long and 9 or 15 μm wide. Due to the different thickness of the palladium layers, the superconducting critical temperature, T_c , resistively measured using a four-contact technique, was 6.3 K for the samples with $d_{\text{Pd}} = 18$ and 20 nm and 7.0 K for the sample with $d_{\text{Pd}} = 1.7$ nm. The width of the resistive transition was always less than 0.1 K in zero field [20].

For comparison Nb/NbO multilayers were also studied. In this case, the samples were deposited on sapphire substrates by magnetron sputtering in a high-vacuum system. The temperature of the sapphire substrates did not exceed 70 °C during the deposition. The samples analyzed in this paper had Nb layer thicknesses of 45 and 90 nm. The critical temperature of a single Nb film was 8.9 K. NbO layers were obtained by oxidation of the Nb film in the deposition chamber. The thickness of the insulator layers in all the samples was 2 nm. The numbers of niobium layers deposited for the first and the second structure were 14 and 10, respectively. Using a photolithographic technique a set of narrow strips was formed on each film. The stripes were 100 μm long while the width of the stripes was 5 or 9 μm .

Magnetization versus temperature measurements, performed using a commercial Quantum Design magnetic properties measurement system (MPMS) SQUID magnetometer, have been done on all the studied samples in the presence of an external magnetic field applied parallel to the layers. The results are presented in figure 1 (for the Nb/Pd sample with $d_{\text{Pd}} = 20$ nm, squares) and (for the Nb/NbO sample with $d_{\text{Nb}} = 90$ nm, circles). From figure 1 it is seen that the onset of the $M(T)$ transition for Nb/Pd at $\mu_0 H = 0.01$ T is close to the one obtained from $R(T)$ measurements, but the width of the phase transition into superconducting state, $\Delta T_c \approx 2$ K, is much larger than the one obtained from resistive measurements [20]. It is worth noting that the curve shows that

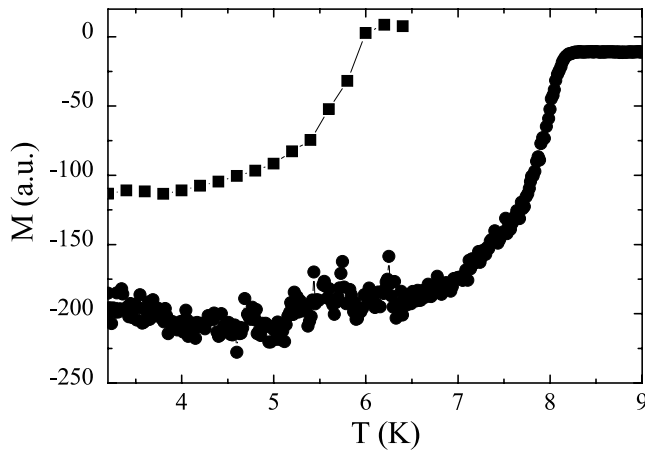


Figure 1. Magnetization versus temperature curves for the Nb/Pd sample with $d_{\text{Pd}} = 20$ nm at $\mu_0 H = 0.01$ T (squares) and for the Nb/NbO sample with $d_{\text{Nb}} = 90$ nm at $\mu_0 H = 0.3$ T (circles).

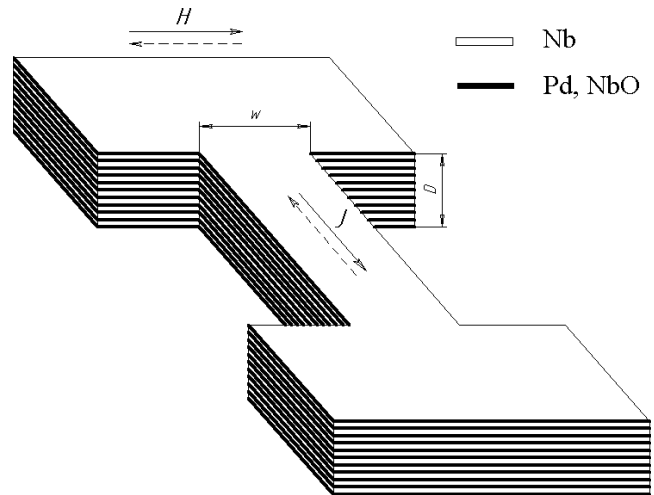


Figure 2. Sketch of the measurement arrangement.

the transition to the superconducting state is not completed at $T = 4.2$ K. This means that, at the temperature at which all the measurements presented in this paper have been performed, superconductivity is only partially present in the Nb layers. The situation is different in the Nb/NbO sample where, despite the much stronger applied magnetic field ($\mu_0 H = 0.3$ T), the transition to the superconducting state is already fully realized for temperatures close to 6 K, which is higher than the working temperature.

Current–voltage characteristics were measured by a standard four-point technique. The critical current was determined as the current at which the voltage drop on a sample reaches $1 \mu\text{V}$. The detection of the critical current in our experiment was fully automated and this allowed the determination of the voltage drop with an accuracy of $0.1 \mu\text{V}$. The $I_c(H)$ dependencies were measured at $T = 4.2$ K with the samples directly in contact with liquid helium. Figure 2 shows a sketch of the measurement method used in our experiments. The distinctive feature of our work is the change of the polarity either of the transport current (which we call positive or negative), which was always applied parallel to the sample surface and perpendicularly to the applied magnetic field, or of the applied magnetic field directed parallel to the sample surface.

3. Results

3.1. Nb/NbO multilayered structures

In figure 3 an example of the field dependencies of the critical current density J_c (figure 3(a)) and the volume pinning force $P_v = \mu_0 H J_c$ (figure 3(b)) obtained on the Nb/NbO sample with $d_{\text{Nb}} = 45$ nm are presented. Points corresponding to positive and negative transport current directions are shown by circles and squares, respectively. Two different measurement methods have been used. In the first method, the polarity of the transport current is changed only after the whole $J_c(H)$ dependence is measured. The same results are obtained if the polarity of the external magnetic field is changed keeping

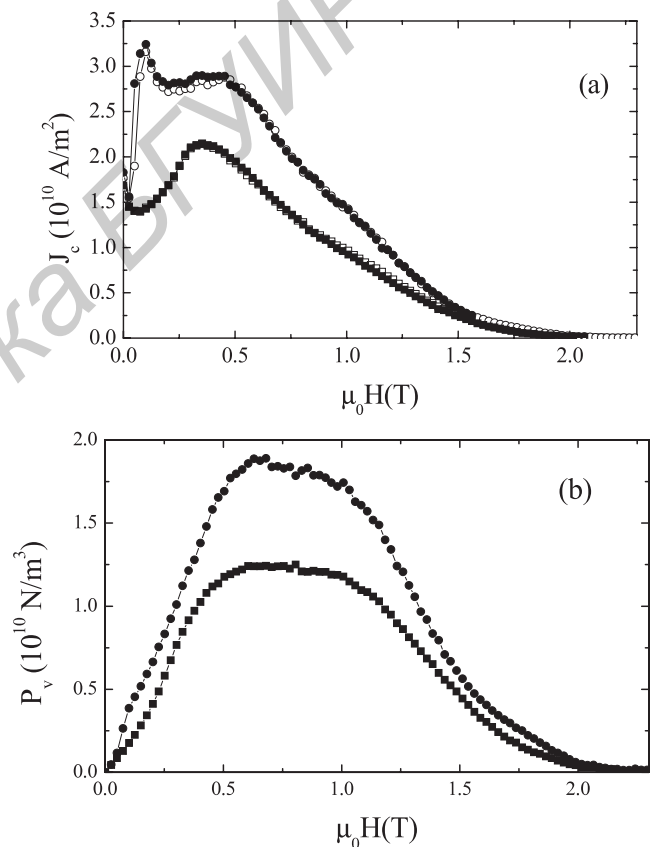


Figure 3. Critical current density (a) and volume pinning force (b) versus external parallel magnetic field for the Nb/NbO sample with $d_{\text{Nb}} = 45$ nm. For this sample $w = 5 \mu\text{m}$. Circles and squares refer to positive and negative directions of the bias current, respectively. Closed and open symbols in (a) correspond to the two measuring methods described in detail in the text.

constant the polarity of the transport current. In the second method, two critical current measurements corresponding to the opposite directions of the transport current were performed in series for each magnetic field value. The obtained $J_c(H)$ curves are independent from the above methods and this indicates that the sample history referred to the previous

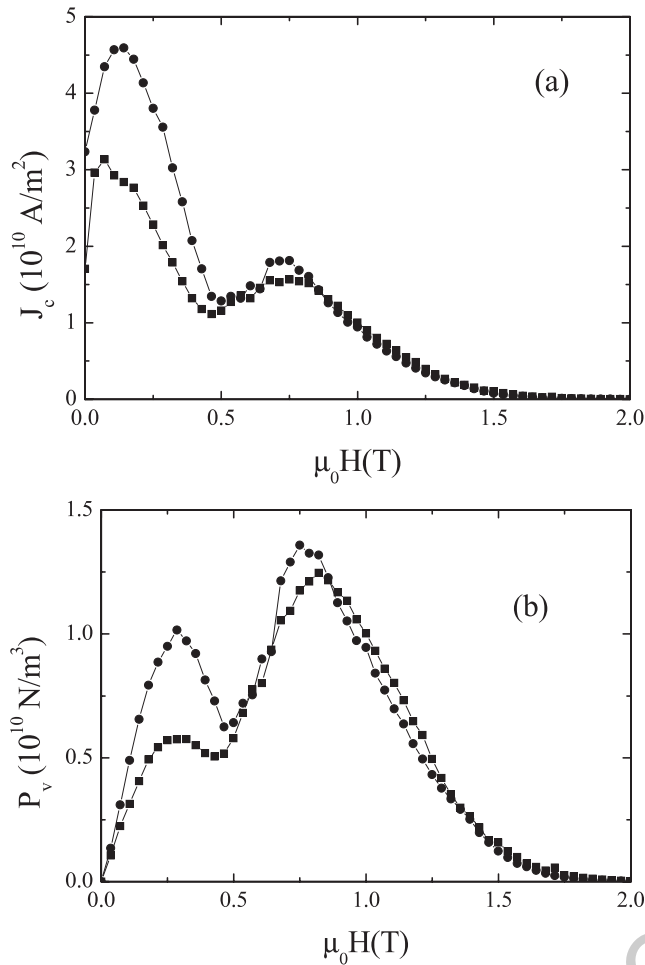


Figure 4. Critical current density (a) and volume pinning force (b) versus parallel external magnetic field for the Nb/NbO sample with $d_{\text{Nb}} = 90$ nm. For this sample $w = 9 \mu\text{m}$. Circles and squares refer to positive and negative directions of the bias current, respectively.

critical current measurements does not affect the results of the experiment. This can be explicitly seen in figure 3(a), where open and solid symbols refer to the two measurement methods: results obtained by the first method are presented by solid symbols while open symbols refer to the second method. Also, we have performed the measurements for an arbitrary sequence of the magnetic field to determine the possible influence of the magnetic history (connected with the magnetic field at the previous points) on the critical current. The experimental evidence reveals that the I_c values were independent of the magnetic field sequence and were determined only by the external magnetic field and by the direction of the transport current in each measurement. In figures 3(a) and (b) a large difference in almost the entire range of magnetic fields is visible in the $J_c(H)$ and $P_v(H)$ dependencies corresponding to the different polarities of the transport current. Another noticeable feature of the $J_c(H)$ dependencies for this sample is the presence of the peak effect for both current directions at $\mu_0 H = 0.35$ T. This value cannot be explained either by matching of the vortex lattice period with the period of the multilayer [11] or by the vortex rearrangement in the whole sample thickness [5]. Also it is worth noting that at low

magnetic field, around 0.11 T, the peak is present in the $J_c(H)$ dependence only for one current direction. Such behavior cannot be explained by the existing theories.

The results for the Nb/NbO sample with $d_{\text{Nb}} = 90$ nm are presented in figure 4. This sample shows a difference in the data for the two polarities of the bias current only at low magnetic fields. Two peaks were observed on the $J_c(H)$ dependencies, at $\mu_0 H \approx 0.1$ and 0.8 T. In the last case the position of the peak does not depend on the direction of the current. The magnetic field value where the second peak is present cannot be explained by the existing theories, see formulae (1) and (2). It is interesting to note that the first peak is observed for both the analyzed Nb/NbO samples at the same magnetic field value, $\mu_0 H \approx 0.1$ T, in spite of the large difference of the periods of the multilayered structures. Also, for the sample with the smaller period this peak is observed only for one direction of the transport current. In conclusion, we can say that both the theoretical approaches based on matching-like arguments [5, 11] are not able to explain the position of the second peak field with increasing period (or the total thickness of the sample) and cannot explain why the position of the first peak does not depend on the period of layering Λ or on the sample thickness D .

3.2. Nb/Pd multilayered structures

The $J_c(H)$ and $P_v(H)$ dependencies for the sample with $d_{\text{Pd}} = 18$ nm are shown in figure 5. Similar dependencies were observed for the sample with $d_{\text{Pd}} = 20$ nm. The dependencies corresponding to both the directions of the transport current are shown also by circles and squares, respectively. First of all, we should note that the critical current density of the Nb/Pd samples and the volume pinning force are close to the corresponding values obtained on the Nb/NbO samples in spite of the fact that the T_c of the Nb/Pd samples is smaller than the critical temperature of the Nb/NbO samples, as is shown in figure 1. This proves that the Pd layers act as effective pinning centers. The $J_c(H)$ dependencies still show very pronounced peaks. The main difference between the dependencies corresponding to the opposite transport current directions is observed at medium magnetic fields near the peak position, while the discrepancy at weak fields is almost absent.

The magnetic field dependencies of the critical current density and the volume pinning force for the sample with the palladium thickness 1.7 nm have also been measured. The results, reported in figure 6, show a difference between the dependencies obtained for positive and negative directions of the transport current only at weak magnetic fields. The $J_c(H)$ dependencies at weak magnetic fields are similar to those observed on Nb/NbO samples at this field range (figures 3(a) and 4(a)). The peak effect is observed near $\mu_0 H = 0.1$ T and only on the $J_c(H)$ curve measured in one direction of the transport current. Finally, at intermediate magnetic fields, the $P_v(H)$ curves show a plateau.

Here we wish to note that the results obtained on Nb/Pd multilayers also do not agree with the present theoretical descriptions. In particular, the magnetic field at which a peak is present in the $J_c(H)$ curves increases with increasing Λ and

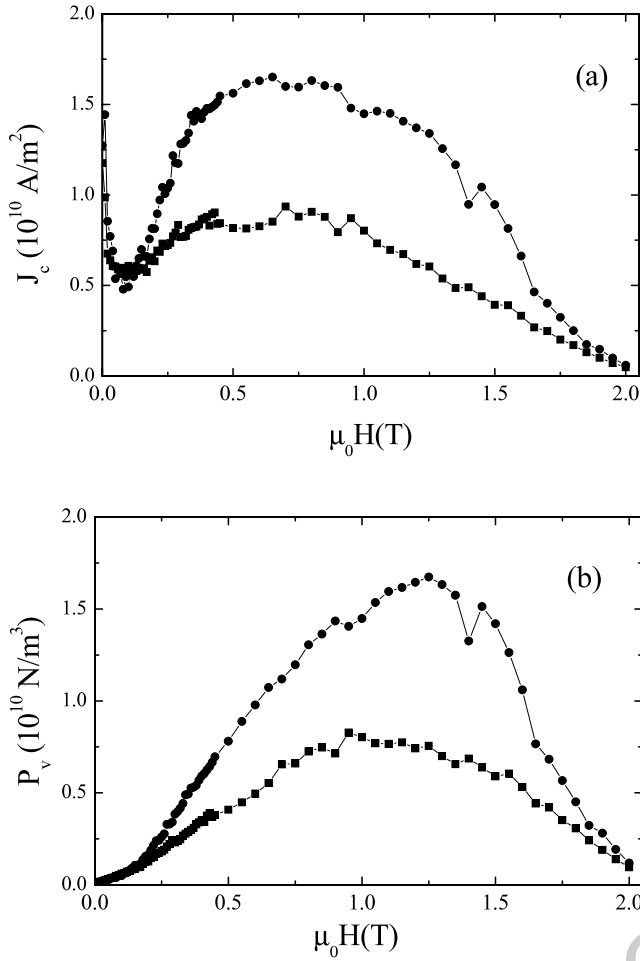


Figure 5. Critical current density (a) and volume pinning force (b) versus parallel external magnetic field for the Nb/Pd sample with $d_{\text{Pd}} = 18$ nm. For this sample $w = 9$ μm . Circles and squares refer to positive and negative directions of the bias current, respectively.

D : this is in contrast to the theoretical predictions for which the matching magnetic field H_m should increase when Λ and D decrease. Moreover, the anisotropy parameter γ evaluated for the Nb/Pd sample with $d_{\text{Pd}} = 18$ nm is larger than the one for the sample with $d_{\text{Pd}} = 1.7$ nm [8]. According to the vortex rearrangement model [5] the matching field should increase when γ decreases, but this fact has not been experimentally observed.

4. Theory

In order to interpret our experimental data we used the approach developed in [19]. We consider a stack of long and wide superconducting plates each of thickness d in a magnetic field H applied parallel to the layers. Each plate carries a transport current perpendicular to the applied field. The transport current I_t is defined as the current density multiplied by the plate thickness, i.e., the current per unit plate width. The calculation of the critical current for this structure is divided into two steps. First, a self-consistent solution of the Ginzburg–Landau equations is used to find the dependence of the critical current I_c on the applied magnetic field strength H for an individual plate, which is assumed to be in the vortex-free

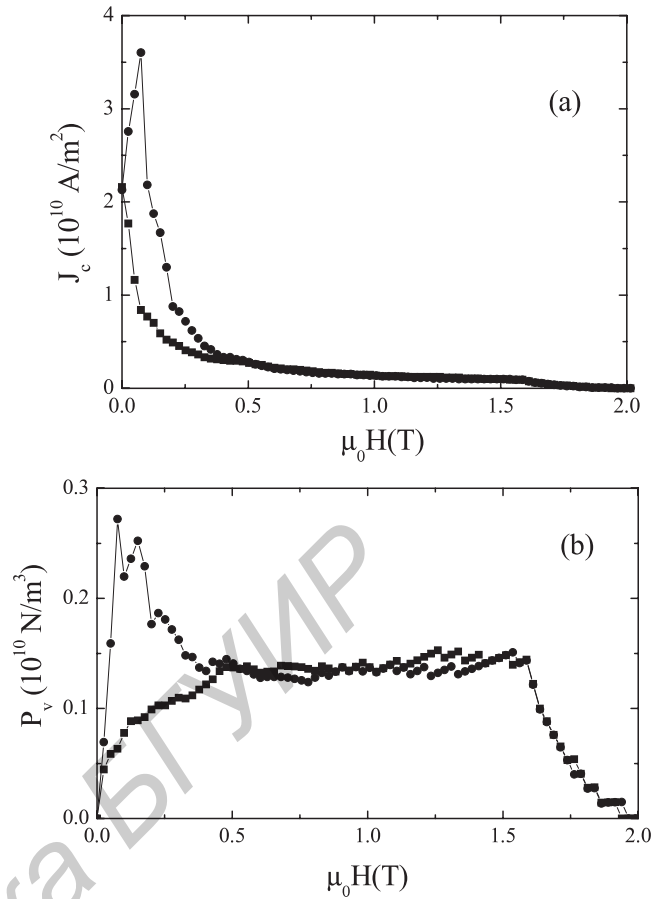


Figure 6. Critical current density (a) and volume pinning force (b) versus parallel external magnetic field for the Nb/Pd sample with $d_{\text{Pd}} = 1.7$ nm. For this sample $w = 15$ μm . Circles and squares refer to positive and negative directions of the bias current, respectively.

state. Second, the critical current is determined for a multilayer by finding an optimal distribution of transport current over individual plates.

We write the Ginzburg–Landau equations in a Cartesian coordinate system (x, y, z) with the y and z axes parallel to the plate surface and the z axis parallel to the magnetic field, assuming that the transport current flows along the y axis. The vector-potential \mathbf{A} has only one component, $\mathbf{A} = \mathbf{e}_y A(x)$. These equations may be written in the dimensionless form:

$$\frac{d^2 U}{dx_\lambda^2} - \psi^2 U = 0, \quad (3)$$

$$\frac{d^2 \psi}{dx_\lambda^2} + \kappa^2 (\psi - \psi^3) - U^2 \psi = 0, \quad (4)$$

where ψ is the superconducting order parameter. We introduce dimensionless quantities U , $b(x_\lambda)$, and $j(x_\lambda)$ instead of the dimensional potential A , magnetic induction B , and current density j_s :

$$A = \frac{\Phi_0}{2\pi\lambda} U, \quad B = \frac{\Phi_0}{2\pi\lambda^2} b, \quad b = \frac{dU}{dx_\lambda}, \quad (5)$$

$$j(x^*) = j_s \left(\frac{c\Phi_0}{8\pi^2\lambda^3} \right)^{-1} = -\psi^2 U, \quad x^* = \frac{x}{\lambda},$$

where $\mathbf{B} = \text{rot } \mathbf{A}$, j_s is the current density, λ is the magnetic field penetration depth and c is the speed of light in a vacuum. Since the transport current I_t carried by the plate generates the magnetic field

$$H_I = \frac{2\pi}{c} I_t, \quad (6)$$

the total field strengths at the plate surfaces are $H \pm H_I$. Accordingly, the following boundary conditions correspond to equation (3):

$$b|_{x^*=0} = h - h_I, \quad b|_{x^*=d^*} = h + h_I, \quad (7)$$

where $h = H/H_\lambda$, $h_I = H_I/H_\lambda$, $d^* = d/\lambda$, $H_\lambda = \frac{\Phi_0}{2\pi\lambda^2}$. Equation (4) is subject to standard boundary conditions on the plate surfaces:

$$\left. \frac{d\psi}{dx^*} \right|_{x^*=0} = 0, \quad \left. \frac{d\psi}{dx^*} \right|_{x^*=d^*} = 0. \quad (8)$$

To find a self-consistent solution of equations (3) and (4), we used the iterative procedure [19].

Proceeding to the second step, we seek the critical current for the multilayer [19]. We assume that there is the relatively thick insulating layer separating the adjacent superconducting layers, i.e., the Josephson coupling between the layers is negligible. To allow for electrical coupling between the superconducting layers, we assume that they are connected by superconducting links at $y = \pm\infty$. This model describes the Nb/NbO multilayer structures well while there are some problems in the case of Nb/Pd multilayers due to the proximity effect in these systems.

We seek such a distribution of transport current over the layers so that the transition to the normal state occurs in all layers simultaneously. If h_i is the magnetic field corresponding to the i th layer, then the current per unit width of the film in the critical state equals the critical current $I_c(h_i)$, which is determined by the numerical solution of the Ginzburg–Landau equations obtained in the first step. Under this condition, each layer in the structure carries a corresponding critical current. The current flowing through the i th plate generates the magnetic field given by (6). According to the field superposition principle, we must add up the contributions of all the layers to find the magnetic field that acts on the i th superconducting layer:

$$h_i = h + \sum_{j=1}^{i-1} h_{tj} - \sum_{j=i+1}^N h_{tj} \quad (9)$$

where h_{tj} is the dimensionless magnetic field generated by the transport current carried by the j th layer. The critical current and magnetic field distribution over the layers that corresponds to their simultaneous transition to the normal state is found using an iterative procedure [19].

This method can be successfully applied to analyze the critical states of multilayers consisting of layers with different properties. This is the case for our samples as is clear from the magnetization measurements. For the Nb/Pd samples with thick palladium layers, $d_{\text{Pd}} = 20$ or 18 nm (see figure 5), palladium suppresses the superconducting properties

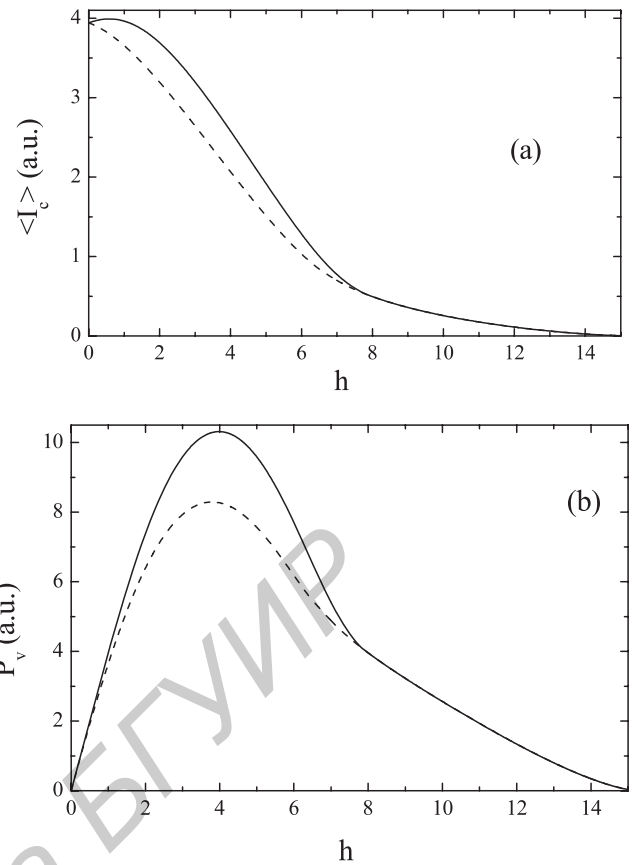


Figure 7. Dependence of the critical current density (a) and the bulk pinning force (b) on the applied parallel magnetic field for a multilayered structure consisting of two types of superconducting layers with different Ginzburg–Landau parameters: for the first five layers $\kappa = 3$ and for the other five layers $\kappa = 2$. The thickness of each layer is the same. Solid (dashed) lines show the dependencies for the positive (negative) direction of the bias current.

of the niobium layers and T_c drops very quickly for $d_{\text{Nb}} < 20$ nm [21]. As a result, even a small deviation of the $\Delta d_{\text{Nb}} \sim 1$ nm can give a T_c variation for the Nb layers of an appreciable quantity. This non-homogeneity of the superconducting properties of the Nb layers can be due, for example, to a small drift of the sputtering parameters during the deposition. To model these differences we can assume that the superconducting layers are characterized by different Ginzburg–Landau parameters, κ . Figure 7(a) shows the behavior of the average current, calculated by using the iterative process described above, as a function of the magnetic field. The simulation in this case has been done considering the multilayer as consisting of two types of superconducting layers with different parameters κ : the first five layers have $\kappa = 3$ while the second ones have $\kappa = 2$. All the layers have the same thickness. In agreement with the experiment, the behavior of $\langle I_c \rangle(h)$ depends on the direction of the transport current, with I_c^+ (corresponding to the positive direction of I_{bias}) and I_c^- (corresponding to the negative direction of I_{bias}) having different values. Also, only one of the two magnetic field dependencies shows a peak (solid line in the figure). It should be noted that the magnetic field dependencies of the J_c of the individual layers, which form the multilayered

structure, are monotonically decreasing functions. Figure 7(b) shows the magnetic field dependencies $P_v(h)$ for the positive and negative directions of the transport current. We can see that the method can explain the observed differences between the $\langle I_c \rangle(h)$ and $P_v(h)$ dependencies which correspond to the opposite directions of the transport current shown in figures 3 and 5 at intermediate magnetic fields. Also, our calculations show that the presence of a peak effect can be explained by taking into account the non-uniformity of the superconducting multilayers without invoking any matching mechanism.

The observed effect is explained by superposition of the applied magnetic field and the field induced by the current flowing along the layers. The transport current induces a magnetic field in the same direction as the applied field on a boundary of the multilayered structure and in the opposite direction on the other boundary. If the current changes its direction, the field also changes its direction. Thus, on the first boundary, the field of the transport current is directed along the external magnetic field and they are additive. On the opposite boundary, the field of the current is directed oppositely to the applied magnetic field and this causes a decrease of the total magnetic field. For homogeneous structures the change in the induced magnetic field has no effect on the $\langle I_c \rangle(h)$ dependence because the structure is symmetric—that is all the layers are identical. On the other hand, for inhomogeneous structures this results in different $\langle I_c \rangle(h)$ dependencies. So, contrary to Kadin's approach [18], our method is able to explain the experimental result that the ratio I_c^+/I_c^- depends on the applied magnetic field. Moreover, when the applied magnetic field is small, the total field in the inhomogeneous sample can be different in the layers close to the non-homogeneity. This causes a higher critical current value for the layers in which the field is smaller and gives a reason for the experimental observation of the peak effect in the $J_c(H)$ curves at small H values.

It is worth noting that even a deviation in the physical properties of only one of the layers can lead to appreciable results. This deviation can be due, for example, to the interaction with the substrate of the first layer or due to contact with air of the last layer in the case of the Nb/NbO multilayers and Nb/Pd multilayers with an extremely small thickness of the Pd layers $d_{Pd} = 1.7$ nm. A result of the simulation for this case is presented in Figures 8(a) and (b), for the average current and for $P_v(h)$ versus the magnetic field for the positive and negative transport current directions, respectively. Calculations were performed for a multilayered structure with ten superconducting layers. The thickness of each layer was equal, but the Ginzburg–Landau parameter κ for the first layer was chosen equal to three, while for other nine layers it was taken equal to one. We can see again that the behavior of $\langle I_c \rangle(h)$ and $P_v(h)$ depends on the direction of the transport current. The theory can also explain the existence of the $J_c(H)$ peak at $\mu_0 H \approx 0.1$ T observed on Nb/NbO multilayers (figures 3(a) and 4(a)) and in the Nb/Pd multilayers with $d_{Pd} = 1.7$ nm (figure 6(a)). In accordance with the experiment, the peak exists only on $J_c(H)$ curves calculated for the positive direction of the transport current.

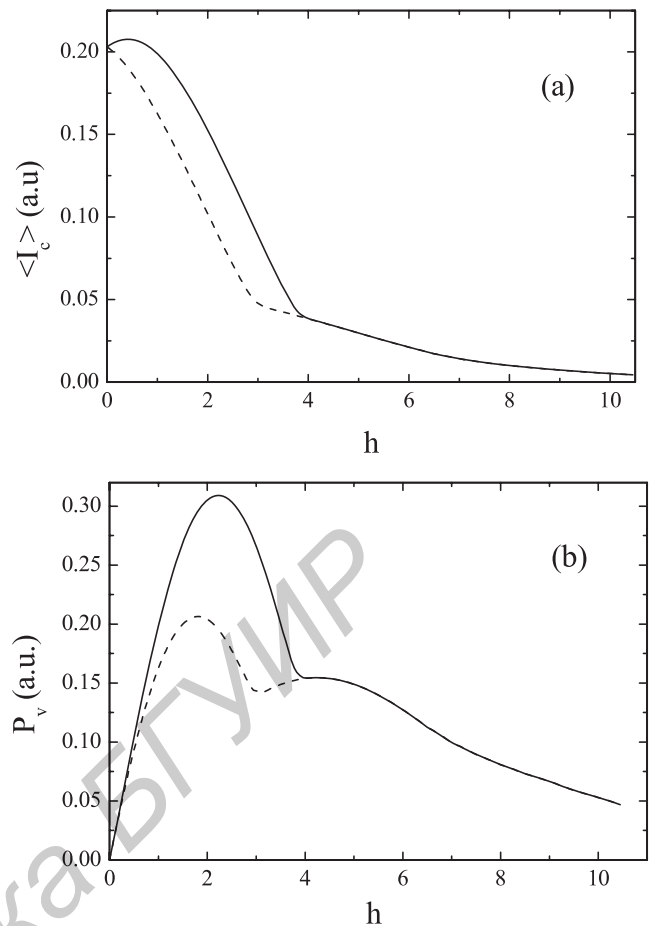


Figure 8. Dependence of the critical current density (a) and the bulk pinning force (b) on the applied parallel magnetic field for a multilayered structure consisting of two types of superconducting layers with different Ginzburg–Landau parameters: for the first layer $\kappa = 3$ and for the other nine layers $\kappa = 1$. The thickness of each layer is the same. Solid (dashed) lines show the dependencies for the positive (negative) direction of the bias current.

Moreover, the $P_v(h)$ dependencies differ drastically from the dependencies for homogeneous multilayers. The main difference is the presence of the two maxima on the curves. For a multilayer consisting of identical layers, only one peak is present. Thus the method can explain the difference between the $\langle I_c \rangle(h)$ and the $P_v(h)$ dependencies corresponding to the opposite transport current directions shown on figures 3, 4 and 6 at low magnetic fields. Similar curves with two maxima were detected in experimental works which investigated the behavior of the pinning force in multilayers [2, 8, 24], where the existence of the additional maximum was explained as due to the matching of the vortex lattice with the layered structure. In our case this results from the current distribution features in inhomogeneous multilayers.

5. Conclusions

In this paper, measurements of the magnetic field dependencies of critical current were performed on Nb/Pd and Nb/NbO multilayer structures in order to study the nature of the peak

effect. The value of the critical current and the presence of the peak in the $I_c(H)$ curves were found to depend on the transport current direction. The experimental results have been explained by considering a numerical method used to analyze the critical state of the superconducting multilayers. The method is based on self-consistent solution of a Ginzburg–Landau system of nonlinear equations which describe the behavior of a superconducting plate carrying a transport current in a magnetic field, provided that there are no vortices inside the plate. The field-dependent critical currents computed for the superconducting layers are used to determine the critical current as a function of the parallel applied magnetic field for the whole layered system. The mutual influence of the superconducting layers is assumed to be realized only via the magnetic field. The experimental results were explained by a superposition of the applied magnetic field and of the field induced by the current flowing along the layers in inhomogeneous superconducting multilayers, which results in the current distribution features in the inhomogeneous multilayers. The method makes it possible to account for the peak effect observed in multilayered superconductors, and can explain the magnetic field dependence of the ratio I_c^+/I_c^- which was detected in the experiment. However the value of the observed peak and of the experimental ratio I_c^+/I_c^- are higher than the corresponding theoretical values. This lack of quantitative agreement between theory and experimental results is probably due the interaction of the vortices with the layer boundaries [8], which were not taken into account in our calculation.

Acknowledgment

This work was in part financially supported by the Program of Russian Academy of Sciences No. 27.

References

- [1] Lykov A N 1993 *Adv. Phys.* **42** 263
- [2] Raffy H, Renard J C and Guyon E 1972 *Solid State Commun.* **11** 1679
- [3] Broussard P R and Geballe T H 1988 *Phys. Rev. B* **37** 68
- [4] Koorevaar P, Maj W, Kes P H and Aarts J 1993 *Phys. Rev. B* **47** 934
- [5] Brongersma S H, Verweij E, Koeman N J, de Groot D G, Griessen R and Ivlev B I 1993 *Phys. Rev. Lett.* **71** 2319
- [6] Ziese M, Esquinzi P, Wagner P, Adrian H, Brongersma S H and Grissen R 1996 *Phys. Rev. B* **53** 8658
- [7] Lobotka P et al 1994 *Physica C* **229** 231
- [8] Coccoresse C et al 1998 *Phys. Rev. B* **57** 7922
- [9] Fogel N Ya et al 2001 *Low Temp. Phys.* **27** 752
- [10] Fogel N Ya, Mikhailov M Yu, Bomze Y V and Yuzepovich O I 1999 *Phys. Rev. B* **59** 3365
- [11] Ami S and Maki K 1975 *Prog. Theor. Phys.* **53** 1
- [12] Kulić M and Dobrosavljević L 1976 *Phys. Status Solidi b* **75** 677
- [13] Kulić M and Rys F S 1989 *J. Low Temp. Phys.* **76** 167
- [14] Kugel K I, Matsushita T, Melikov E Z and Rakhmanov A I 1994 *Physica C* **228** 373
- [15] Kushnir V N, Prischepa S L, Attanasio C and Maritato L 2001 *Phys. Rev. B* **63** 092503
- [16] Brongersma S H, Verweij E, Koeman N Y, de Groot D G and Griessen R 1993 *Thin Solid Films* **228** 201
- [17] Bean C P and Livingston J D 1964 *Phys. Rev. Lett.* **12** 11
- [18] Kadin A M, Burkhardt R W, Cheb J T, Keem J E and Oyshinsky S R 1984 *Proc. 17th Int. Conf. on Low Temp. Phys.* p C09
- [19] Lykov A N and Tsvetkov A Yu 2007 *Phys. Rev. B* **76** 144517
- [20] Cirillo C, Attanasio C, Maritato L, Mercaldo L V, Prischepa S L and Salvato M 2003 *J. Low Temp. Phys.* **130** 509
- [21] Cirillo C, Prischepa S L, Salvato M and Attanasio C 2004 *Eur. Phys. J. B* **38** 59
- [22] Lykov A N 2009 private communication
- [23] Potenza A, Gabureac M S and Marrows C H 2007 *Phys. Rev. B* **76** 014534
- [24] Kushnir V N, Petrov A Yu, Prischepa S L, Attanasio C and Maritato L 2001 *Proc. 10th Int. Workshop on Critical Currents* ed C Jooss, p 184